Forming-free resistive switching of tunable ZnO films grown by atomic layer deposition

Ruomeng Huang*, Kai Sun, Kian S. Kiang, Katrina A. Morgan, and C. H. de Groot

School of Electronics and Computer Science, University of Southampton, SO17 1BJ, UK

Abstract

Undoped ZnO thin films with tunable electrical properties have been achieved by adjusting the O_2 plasma time in the plasma enhanced atomic layer deposition process. The structural, compositional and electrical properties of the deposited ZnO films were investigated by various characterization techniques. By tuning the plasma exposure from 2 to 8 s, both resistivities and carrier concentrations of the resultant ZnO films can be modulated by up to 3 orders of magnitude. Forming-free TiN/ZnO/TiN resistive memory devices have been achieved by choosing the ZnO film with the plasma exposure time of 6 s. This deposition method offers a great potential for producing other un-doped metal oxides with tunable properties as well as complex multilayer structures in a single deposition.

Keywords

ZnO, atomic layer deposition, forming-free, resistive memory

1. Introduction

The ever increasing demand for the universal memory is driving the development of new memory concepts and materials. Among the many contenders for the next-generation of memory device, resistive switching memory based on metal oxides has emerged as the leading candidate [1]. Many metal oxides have been reported to show resistive switching properties such as TiO_2 [2], HfO_2 [3,4], Ta_2O_5 [5] etc. For resistive memory in general, high-voltage forming process is needed to initiate the switching, which will normally lead to high power consumption and increased circuit and operational complexity [1]. The development of forming-free resistive memory devices is therefore desirable. As the requirement for a high forming voltage is primarily due to the initial insulating or high resistive state of the oxide materials, being able to tune electrical properties of the as-deposited metal oxide layer could therefore be beneficial in achieving forming-free RS memory.

ZnO has been widely used in a range of electronic and optoelectronic applications due to its excellent optical and electrical properties [6]. It also demonstrates excellent resistive switching characteristics [7–9], making it a suitable candidate for RS memory. Modulating the electrical properties of the as-deposited ZnO films is usually achieved by doping [10,11]. However, doping typically requires modified source materials and could be difficult to control and reproduce. Modulation of the electrical properties of undoped-ZnO by a single deposition process can therefore be advantageous.

In this work, we demonstrate the modulation of ZnO film electrical properties by plasma enhanced atomic layer deposition (PE-ALD). ALD has been established as an excellent method in fabricating RS memory devices [12]. Comparing with the conventional thermal ALD, PE-ALD offers better process control which facilitates the modulation of the resultant film properties. In this work, O_2 plasma time is adjusted and proved to be an effective factor in modulating the ZnO film properties. Structural, electrical and compositional characterization results are presented for ZnO films deposited with

different O_2 plasma times. In addition, forming-free resistive switching of the TiN/ZnO/TiN memory device is presented by carefully choosing the initial resistive state of the as-deposited ZnO film. *I–V* transport properties for both ON-state and OFF-state have been systematically studied with a view to investigating their respective switching mechanisms.

2. Experiment

2.1 ZnO film deposition

All ZnO thin films were prepared in an OIPT FlexAl ALD system using Diethylzinc (DEZ) precursor and O_2 plasma. Within each cycle of the ALD process, the DEZ was introduced to the chamber (DEZ pulse) and subsequently purged using argon (DEZ purge). Immediately after the DEZ pulse and purge, O_2 was flowed into the chamber and the formed O_2 plasma converted the DEZ products into ZnO (O_2 plasma time). The specific details for one growth cycle in the ALD process are given in Table 1.The control of the ZnO film properties was achieved by varying the O_2 plasma time. In this work, four different O_2 plasma times were investigated and all ZnO films were deposited on the SiO_2 coated Si substrates.

Parameter	Condition
DEZ pulse (ms)	60
DEZ purge (s)	4
O_2 plasma time (s)	2, 4, 6, 8
O_2 plasma power (W)	300
O_2 plasma pressure (mT)	15
Temperature (°C)	190

Table 1. Process details for one growth cycle in the ALD process used in this study.

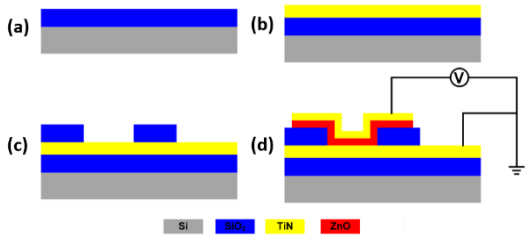

Figure 1. (a–d) Schematic drawings of fabrication process flow for the TiN/ZnO/TiN resistive memory devices, with (d) also showing the electric connection configuration during the switching tests.

2.2 Film characterization

The thickness of the deposited ZnO films was measured by ellipsometry (VASE, J.A. Woollam Co. M-2000) and fitted with a Cauchy-model. The electrical properties were measured by Hall measurements (Nanometrics HL5500PC) at room temperature under a magnetic field of 0.5 Tesla. X-ray diffraction (XRD) patterns were collected in grazing incidence ($\theta_1 = 1^o$) using a Rigaku Smartlab diffractometer with a 9 kW Cu-K_α source. X-ray photoelectron spectroscopy (XPS) data were obtained using a Thermo Scientific Theta Probe System with Al–K_α radiation (photon energy = 1486.6 eV). Where necessary, surface contamination was eliminated by the use of an ion sputtering gun. The Zn 2p, O 1s, and C 1s spectra were collected. All data were referenced to the C 1s peak, which was assigned a binding energy of 284.6 eV. Scanning electron microscopy (SEM) measurements were carried out with a field emission SEM (Jeol JSM 7500F) at an accelerating voltage of 2 kV to observe the film morphologies.

2.3 Memory device fabrication and characterization

The resistive switching behavior of the ZnO film was investigated by fabricating memory devices. The fabrication process is shown in Figure 1. A 200 nm thick TiN film was reactively sputtered (Ti target in a N_2 atmosphere) onto the SiO_2 layer to form the bottom electrode. This was followed by reactive sputtering of a second SiO_2 layer (Si target in an O_2 atmosphere). This layer of SiO_2 was patterned to form active device areas by photolithography and reactive ion etch. Subsequently, a 40 nm ZnO layer was deposited by ALD to form the switching layer. Finally, a 200 nm TiN layer was sputtered and

patterned on the ZnO layer to form the top electrode. All electrical measurements were performed with a Keithley 4200 semiconductor characterization system. During the measurements, the programming voltage bias was applied to the top electrode, while keeping the bottom electrode grounded. The probe/point contacts to the top and bottom electrodes of the devices were realized through a pair of Wentworth probe needles, using a Wentworth laboratories AVT 702 semi-automatic prober. Current compliance was applied during the SET cycles to prevent permanent breakdown.

3. Results and discussion

3.1 ZnO thin films

Figure 2 shows the ZnO growth rates for the ALD process with different O_2 plasma times. The growth rate is found to be quite sensitive to the O_2 plasma at short plasma times where the growth rate increases from *ca.* 1.4 – 1.7 Å/cycle as the plasma time is increased from 2 to 4 s. The growth rate saturates at a level around 1.7 Å /cycle at longer plasma times. This suggests the film growth becomes self-limited, indicating an ALD growth.

All ZnO films were found to be polycrystalline as-deposited as shown in the XRD patterns in Figure 3. Strong (0 0 2) preferred orientation was observed for all four films, consistent with other reported works [13,14]. However, this *c*-axis preferred orientation decreases gradually with the increasing O_2 plasma time, as indicated by the slow increase of the (1 0 0), (1 0 1) and (1 0 2) peaks. The average grain size of the film was estimated using the Debye-Scherrer formula [15]. Similar grain size of *ca.* 19 nm was calculated from the (0 0 2) peak for all four ZnO films, suggesting the ZnO grain size was barely affected by the O_2 plasma time. Cross-sectional SEM images are shown in Figure 4 where similar morphologies for can be observed for all films.

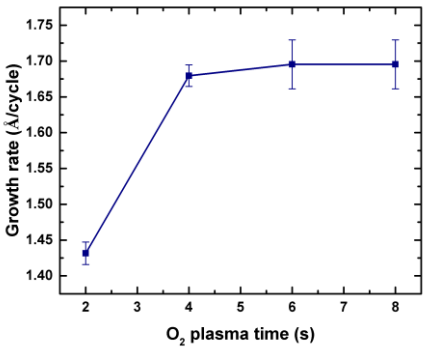

Figure 2. ZnO growth rate as a function of O_2 plasma time.

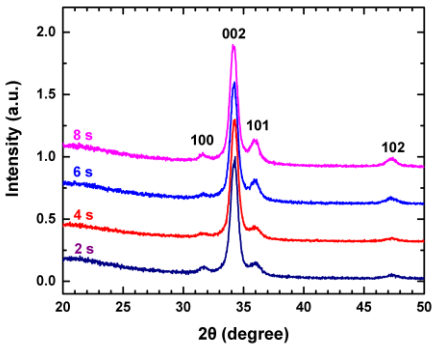

Figure 3. XRD spectra of ZnO thin films deposited with different O_2 plasma times. Spectra are offset and normalized to the (0 0 2) peak.

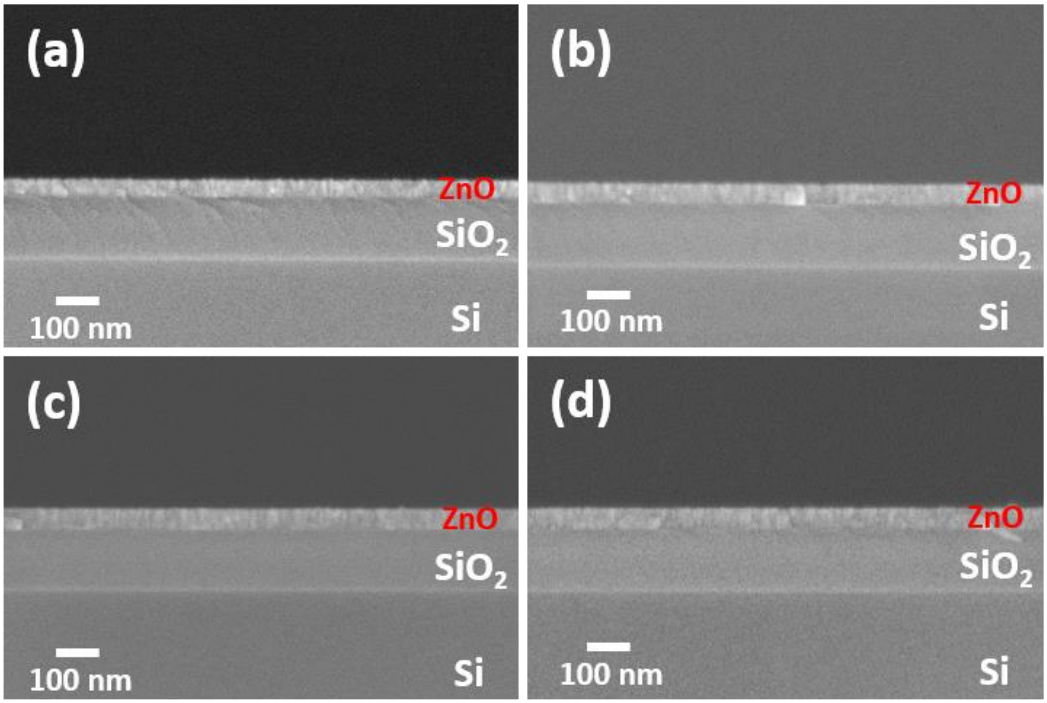

Figure 4. Cross-sectional SEM images of ZnO films grown by PE-ALD with O_2 plasma time of 2 s, 4 s, 6 s and 8 s, respectively.

The effect of the O_2 plasma time on the stoichiometry of the ZnO films was investigated by XPS and the O:Zn ratios are presented in Figure 5a. A range from *ca.* 0.90 to 0.94 was observed which corresponds well with other reported ZnO films deposited by ALD with plasma treatment [16]. In addition, all films exhibit relatively good stoichiometry compared to the ZnO films deposited from thermal ALD [12,16]. This is due to the fact that O_2 plasma is much more reactive than H_2O [12]. In addition, the oxygen concentration increases monotonically with the increase of plasma exposure, indicating that longer O_2 plasma times result in more complete oxidization. Figures 5b-e show the XPS spectra of the O 1s peak and their Gaussian fitting results for all four ZnO films. Three oxygen peaks are featured in all spectra. The main peak at the lowest binding energy (*ca.* 530.3 eV) is typically attributed to the Zn-O bond, indicating the measure of the amount of oxygen atoms in a fully oxidized surrounding [17–19]. Another peak at *ca.* 532.3 eV can be interpreted as the O-H bond, which is typically produced in each half ALD-cycle [17,16,20]. A similar bond was also reported in the PE-ALD of other metal oxides such as Al_2O_3 [21]. A reduction of this peak was observed with increasing O_2 plasma exposure as shown in Figure 5f. The reduction of the O-H peak is accompanied by a significant increase of the third peak at *ca.* 531.3 eV which can be assigned to the oxygen interstitial (O_2^{2-}) [17,16,20]. This suggests that more O_2^{2-} or V_O defects are generated with longer O_2 plasma times while the formation of both the stoichiometric Zn-O bond and the O-H bond are suppressed.

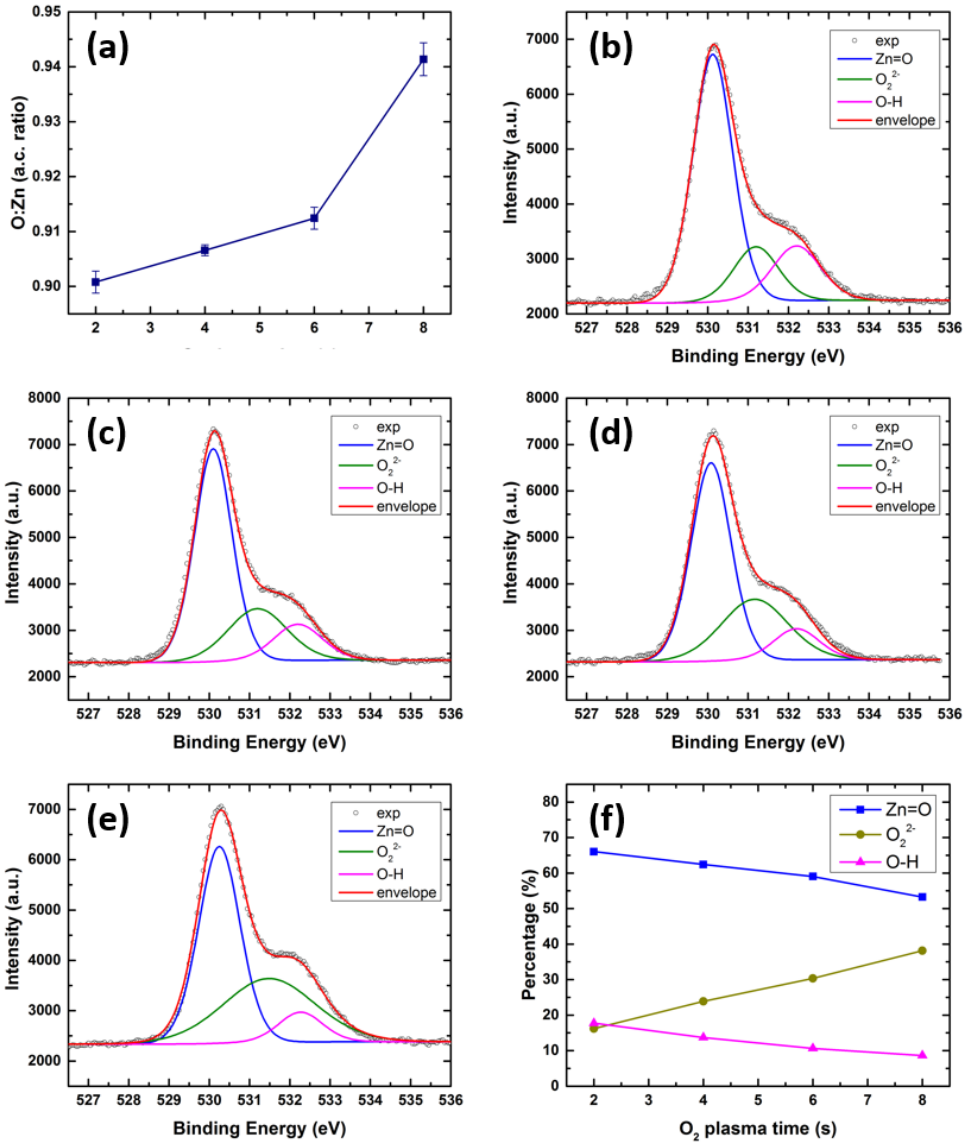

Figure 5. (a) O:Zn atomic concentration ratio in the resultant ZnO films deposited by PEALD as a function of O_2 plasma time; XPS spectra and their Gaussian fittings of the O 1s region with O_2 plasma times of 2 s (b), 4 s (c), 6 s (d) and 8 s (e); (f) Percentages of the fitted peaks of the Zn=O bond, oxygen interstitial and the O-H bond as a function of O_2 plasma time.

Hall measurements revealed that all ZnO films deposited in this work were *n*-type, in correspondence with other reported works [12]. It is believed this *n*-type conductivity originates from the presence of the defects and impurities in the ZnO crystal. Significant change of film resistivity and carrier density was observed as shown in Figure 6. The resistivity increases continuously from *ca.* 2 to 1000 Ω·cm as the O_2 plasma time is increased from 2 to 8 s. In general, high quality and strictly stoichiometry ZnO film is highly insulating. The trend of resistivity increasing with the plasma exposure duration in this work can be associated with the decrease of free electron concentrations. Either the oxygen interstitial or the hydroxyl bond could be the cause. The latter is in agreement with the trend observed in Figure 5f as the concentration of the hydrogen related O-H bonds decreases with the increasing plasma time. It is reported that both hydrogen and hydroxyl in ZnO behave as shallow donors and can lead to higher carrier concentration [22,23]. The reduction of the O-H bond concentration also leads to the decrease of the carrier concentrations presented in Figure 6. On the other hand, the increasing trend of oxygen interstitial concentrations shown in Figure 5f suggests that the effect of oxygen

interstitials on the carrier concentration is not prominent. In fact, theoretical calculations revealed that oxygen vacancies in ZnO form a deep fully occupied state and cannot be a source of free electron [24,25]. The electron mobilities of all four ZnO films were found to be similar (ca. 2.5±0.5 $cm^2/V{\cdot}s$), suggesting the electron mobility is not affected by the plasma exposure duration. The tuning of ZnO films within a 3-order of magnitude resistivity window in this work provides great potential for achieving resistive switching memory devices with optimized performance.

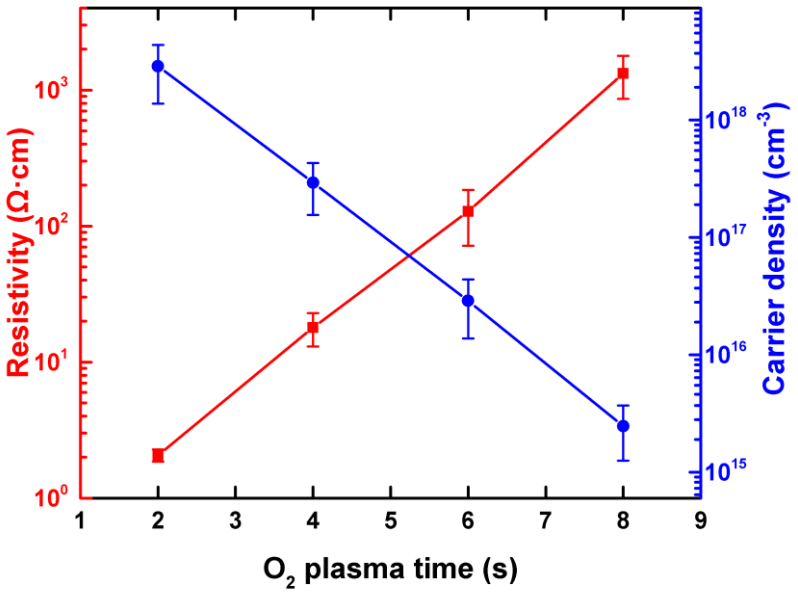

Figure 6. Resistivity and carrier density of the deposited ZnO films as a function of O_2 plasma time.

3.2 ZnO resistive switching memory

Resistive switching in metal oxide resistive memory is achieved by the forming and rupture of the conductive filament [1]. A forming process is required to initiate the filament in the pristine device if the as-deposited oxide layer is highly insulating. On the other hand, a conductive as-deposited oxide layer will normally have no switching behavior due to a large leakage current [14,18]. In this work, ZnO memory device with film resistivity higher than 10^3 Ω·cm resulted in a forming voltage more negative than -8 V. Device with lower film resisitivity (<10 Ω·cm) was found to be Ohmic conducting with no switching behavior. An intermediate-state as-deposited ZnO film is required to achieve the forming-free behavior and therefore the ZnO film grown with 6 s O_2 plasma time was selected and fabricated into the TiN/ZnO/TiN memory device. Typical *I*–*V* characteristics for the first and subsequent SET/RESET switching cycles are shown in Figure 6 with the voltage sweep sequence indicated by the arrows. The device displays bipolar switching behavior where the device is SET at negative bias while RESET at positive bias. The pristine device displays a relative high resistance as the voltage sweeps from 0 to -5 V. A sudden resistance decrease from high resistance state (HRS) to low resistance state (LRS) was observed at about -4 V (SET process). This LRS was maintained as the applied voltage swept back to 0. Sweeping from 0 to 3 V saw the sudden increase of the resistive from LRS to HRS at about 3 V (RESET process). The subsequent SET process resulted in the same negative SET voltage as the first sweep, indicating the forming-free characteristic of this device. However, it is noticeable that, although with the same SET voltage, the I-V characteristics are different between the first and the subsequent sweeps in the SET process.

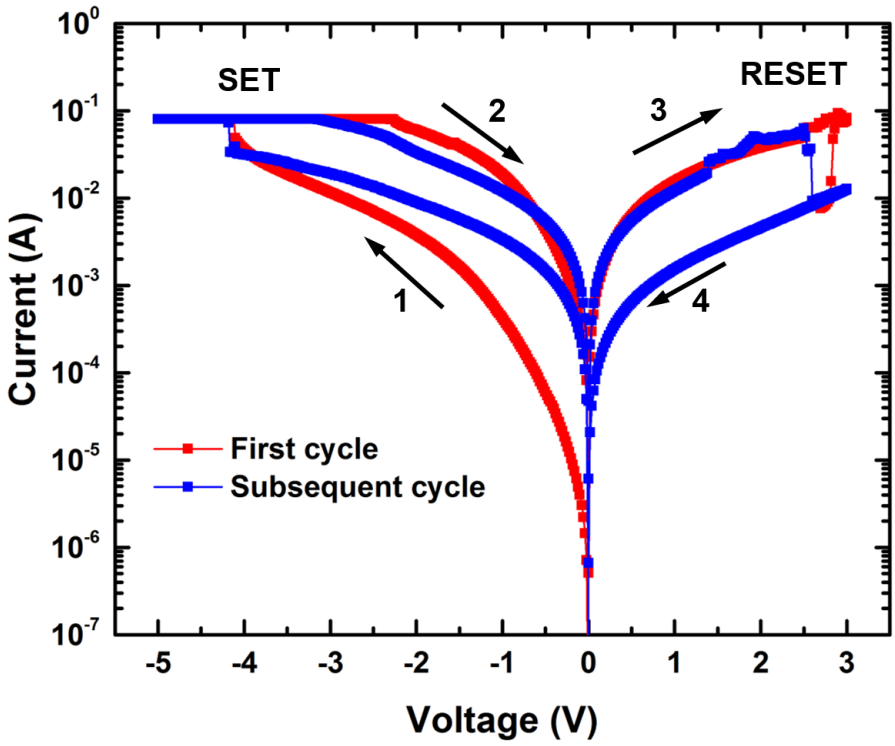

Figure 7. Typical I-V characteristics of the forming-free TiN/ZnO/TiN resistive switching devices. The resistance is changed from HRS to LRS at -4 V (SET) and changed from LRS to HRS at 3 V (RESET).

In order to better understand the conduction mechanisms of the ZnO resistive memory (in Figure 7), the *I–V* characteristics were investigated in detail. Figure 8a depicts the *I-V* curves of the SET process in a double logarithmic plot with linear fits for both first and subsequent cycles. The forming curve of the pristine device suggests the current is governed by the space charge limited current (SCLC) model with traps, which consists of three regions: Ohmic region ($I \propto V$), the Child's law region ($I \propto V^2$) and the steep current increase region, as demonstrated by the different slopes of the linear fits [16,26–28]. In the low voltage region, the curve of Log(I)-Log(V) is linear with the gradient near unity, indicating Ohmic conduction ($I \propto V$). In this region, the density of thermally generated electrons inside the films is larger than the injected electrons from the electrode. As the voltage increases, the slope changes to around 2, indicating the space charge limited current dominates. This occurs when the thermally generated charge concentration is negligible compared to the injected charge concentration. A further increase of the voltage results in the change of conduction mechanism to the trap-filled limited current conduction. This is characterized by a steep current increase (Slope > 2) as the density of occupied trap sites approaches the density of trap levels. It is suggested that within this region, the injected electrons are partly captured by the traps in the films, while others contribute to the total current [28,29]. Comparing with the first cycle, the *I-V* curve of the subsequent switching is featured by only two regions which corresponds well with the trap-free SCLC model [30]. The absence of this region in the subsequent switching implies that traps in the films have been filled during the pristine SET process.

Figure 8b shows the typical *I-V* curves of the RESET process in double logarithmic plot with linear fits. Both first and subsequent RESET display similar features with the LRS well fitted to the Ohmic conduction.

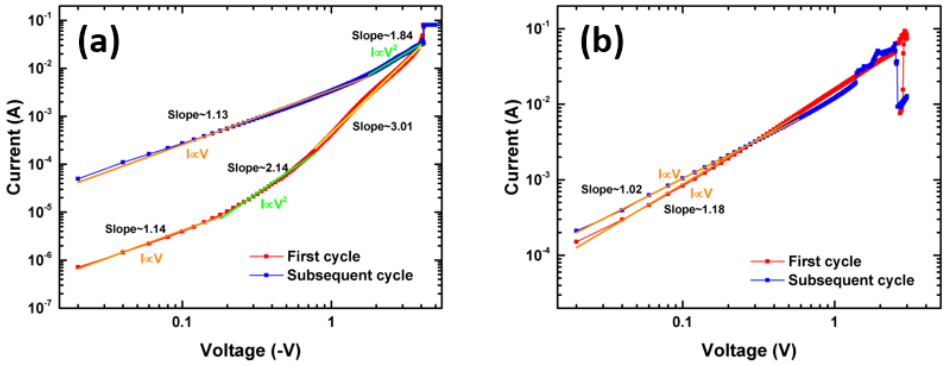

Figure 8. Typical *I-V* curves of the (a) SET and (b) RESET processES in double logarithmic plot with linear fittings for both first (red) and subsequent (blue) switchings.

The filamentary model has been widely accepted to be responsible for the resistive switching behavior of the ZnO-based memory device. Conductive filament made of oxygen vacancies are formed during the SET process when the oxygen ions are forced to migrate to the electrode by the applying voltage. In this work, the oxygen ions migrate only to the bottom electrode and cause the bipolar behavior, despite the symmetric device structure. This is possibly due to the formation of an interfacial TiON layer at the interface between the metal oxide layer and the bottom TiN electrode which serves as an oxygen reservoir [31]. Similar bipolar switching behavior was also observed in HfO_2 in the same device structure [32]. The formation of this filament switches the device from HRS to LRS. At the RESET process, the oxygen ions at the bottom electrode are pushed back to by the opposite RESET bias and react with the vacancies near the electrode. The filament is then broken and the device is switched from LRS back to HRS.

The variations of the resistive switching parameters for the ZnO devices tested in this work are shown in Figure 9a. All parameters display narrow distributions, indicating the good reliability of the fabricated devices. Similar distribution between the $V_{SET\text{-}first}$ and $V_{SET\text{-}subsequent}$ (*ca.* -4 V) suggests the forming-free property of the device. An ON/OFF ratio larger than 10 was also observed, which is sufficiently enough for the memory application. To further analyze the switching performance, retention measurements were carried out at room temperature, as shown in Figure 9b. For both HRS and LRS, no electrical power was required to maintain the resistive states. Both resistances show no sign of deterioration up to 10^4 s, implying that our fabricated device possesses a good retention property.

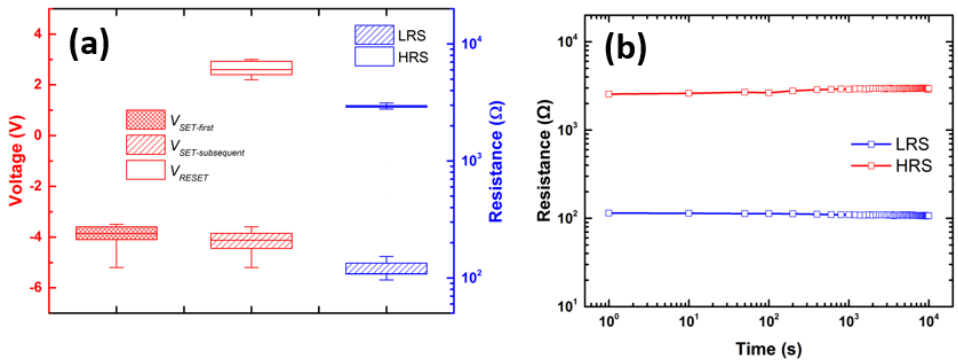

Figure 9. (a) The parameter statistics, including of the $V_{SET\text{-}first}$, $V_{SET\text{-}subsequent}$, V_{RESET}, HRS and LRS of the forming-free TiN/ZnO/TiN resistive switching devices; (b) The retention test of the HRS and LRS after the REST and SET processes, respectively, readout at 0.1 V.

4. Conclusion

This work has demonstrated a modulation technique of tuning ZnO electrical properties through adjusting the O_2 plasma time in the PE-ALD process. The as-deposited ZnO films have shown tunable resistivities with 3 orders of magnitude difference between an O_2 plasma time of 2 and 8 s. All ZnO films are crystalline as-deposited with a preferred orientation in the (0 0 2) direction. XPS results show an increase in oxygen concentration in the ZnO film with longer O_2 plasma time. The RS device based on the ZnO with a 6 s O2 plasma time has exhibited a forming-free characteristic which is highly preferred for RS memory. The RS device demonstrates a bipolar switching behavior with good retention property. Both HRS and LRS conductions are governed by the SCLC model. However, an additional steep current increase step is required in the pristine SET (forming) process.

The deposition of ZnO films with highly tunable properties reported here clearly points towards the capability of transferring this technique to other un-doped metal oxides for tunable properties as well as complex multilayer structures in a single deposition.

Acknowledgement

We thank the EPSRC for support (EP/J002968/1) and for a Doctoral Prize (R.H. EP/509015FP/1).

References

[1] H.-S.P. Wong, H.-Y. Lee, S. Yu, Y.-S. Chen, Y. Wu, P.-S. Chen, et al., Metal–Oxide RRAM, Proc. IEEE. 100 (2012) 1951–1970. doi:10.1109/JPROC.2012.2190369.

[2] D.-H. Kwon, K.M. Kim, J.H. Jang, J.M. Jeon, M.H. Lee, G.H. Kim, et al., Atomic structure of conducting nanofilaments in TiO_2 resistive switching memory., Nat. Nanotechnol. 5 (2010) 148–53. doi:10.1038/nnano.2009.456.

[3] S. Privitera, G. Bersuker, B. Butcher, a. Kalantarian, S. Lombardo, C. Bongiorno, et al., Microscopy study of the conductive filament in HfO_2 resistive switching memory devices, Microelectron. Eng. 109 (2013) 75–78. doi:10.1016/j.mee.2013.03.145.

[4] P.-S. Chen, Y.-S. Chen, K.-H. Tsai, H.-Y. Lee, Polarity dependence of forming step on improved performance in Ti/HfO_x/W with dual resistive switching mode, Microelectron. Eng. (2013). doi:10.1016/j.mee.2013.04.005.

[5] M.-J. Lee, C.B. Lee, D. Lee, S.R. Lee, M. Chang, J.H. Hur, et al., A fast, high-endurance and scalable non-volatile memory device made from asymmetric $Ta_2O_{(5-x)}$/$TaO_{(2-x)}$ bilayer structures., Nat. Mater. 10 (2011) 625–30. doi:10.1038/nmat3070.

[6] D.C. Look, Recent advances in ZnO materials and devices, Mater. Sci. Eng. B Solid-State Mater. Adv. Technol. 80 (2001) 383–387. doi:10.1016/S0921-5107(00)00604-8.

[7] N. Xu, L.F. Liu, X. Sun, C. Chen, Y. Wang, D.D. Han, et al., Bipolar switching behavior in TiN/ZnO/Pt resistive nonvolatile memory with fast switching and long retention, Semicond. Sci. Technol. 23 (2008) 075019. doi:10.1088/0268-1242/23/7/075019.

[8] J. Zhang, H. Yang, Q. Zhang, S. Dong, J.K. Luo, Bipolar resistive switching characteristics of low temperature grown ZnO thin films by plasma-enhanced atomic layer deposition, Appl. Phys. Lett. 102 (2013) 012113. doi:10.1063/1.4774400.

[9] M.H. Tang, B. Jiang, Y.G. Xiao, Z.Q. Zeng, Z.P. Wang, J.C. Li, et al., Top electrode-dependent resistance switching behaviors of ZnO thin films deposited on Pt/Ti/SiO_2/Si substrate, Microelectron. Eng. 93 (2012) 35–38. doi:10.1016/j.mee.2011.12.003.

[10] G. Chen, C. Song, C. Chen, S. Gao, F. Zeng, F. Pan, Resistive switching and magnetic

modulation in cobalt-doped ZnO., Adv. Mater. 24 (2012) 3515–20. doi:10.1002/adma.201201595.

[11] D. Xu, Y. Xiong, M. Tang, B. Zeng, Coexistence of the bipolar and unipolar resistive switching behaviors in vanadium doped ZnO films, J. Alloys Compd. 584 (2014) 269–272. doi:10.1016/j.jallcom.2013.09.073.

[12] T. Tynell, M. Karppinen, Atomic layer deposition of ZnO: a review, Semicond. Sci. Technol. 29 (2014) 043001. doi:10.1088/0268-1242/29/4/043001.

[13] D. Kim, H. Kang, J.-M. Kim, H. Kim, The properties of plasma-enhanced atomic layer deposition (ALD) ZnO thin films and comparison with thermal ALD, Appl. Surf. Sci. 257 (2011) 3776–3779. doi:10.1016/j.apsusc.2010.11.138.

[14] J. Zhang, H. Yang, Q. Zhang, S. Dong, J.K. Luo, Structural, optical, electrical and resistive switching properties of ZnO thin films deposited by thermal and plasma-enhanced atomic layer deposition, Appl. Surf. Sci. 282 (2013) 390–395. doi:10.1016/j.apsusc.2013.05.141.

[15] B.S. Li, Y.C. Liu, Z.Z. Zhi, D.Z. Shen, Y.M. Lu, J.Y. Zhang, et al., Effect of the growth temperature on ZnO thin films grown by plasma enhanced chemical vapor deposition, Thin Solid Films. 414 (2002) 170–174. doi:10.1016/S0040-6090(02)00491-1.

[16] J. Zhang, H. Yang, Q. Zhang, H. Jiang, J. Luo, J. Zhou, et al., Resistive switching of in situ and ex situ oxygen plasma treated ZnO thin film deposited by atomic layer deposition, Appl. Phys. A. (2014). doi:10.1007/s00339-014-8324-4.

[17] M. a Thomas, J.B. Cui, Highly tunable electrical properties in undoped ZnO grown by plasma enhanced thermal-atomic layer deposition., ACS Appl. Mater. Interfaces. 4 (2012) 3122–8. doi:10.1021/am300458q.

[18] F. Zhang, X. Li, X. Gao, L. Wu, F. Zhuge, Q. Wang, et al., Effect of defect content on the unipolar resistive switching characteristics of ZnO thin film memory devices, Solid State Commun. 152 (2012) 1630–1634. doi:10.1016/j.ssc.2012.04.073.

[19] S. Bang, S. Lee, J. Park, S. Park, Y. Ko, C. Choi, et al., The effects of post-annealing on the performance of ZnO thin film transistors, Thin Solid Films. 519 (2011) 8109–8113. doi:10.1016/j.tsf.2011.05.048.

[20] E. Guziewicz, M. Godlewski, L. Wachnicki, T. a Krajewski, G. Luka, S. Gieraltowska, et al., ALD grown zinc oxide with controllable electrical properties, Semicond. Sci. Technol. 27 (2012) 074011. doi:10.1088/0268-1242/27/7/074011.

[21] J. Haeberle, K. Henkel, H. Gargouri, F. Naumann, B. Gruska, M. Arens, et al., Ellipsometry and XPS comparative studies of thermal and plasma enhanced atomic layer deposited Al_2O_3-films, Beilstein J. Nanotechnol. 4 (2013) 732–742. doi:10.3762/bjnano.4.83.

[22] M.J. Jin, J. Jo, G.P. Neupane, J. Kim, K.S. An, J.W. Yoo, Tuning of undoped ZnO thin film via plasma enhanced atomic layer deposition and its application for an inverted polymer solar cell, AIP Adv. 3 (2013) 0–12. doi:10.1063/1.4825230.

[23] L. Zhang, Y. Jiang, Y. Ding, M. Povey, D. York, Investigation into the antibacterial behaviour of suspensions of ZnO nanoparticles (ZnO nanofluids), J. Nanoparticle Res. 9 (2007) 479–489. doi:10.1007/s11051-006-9150-1.

[24] F. Oba, S.R. Nishitani, S. Isotani, H. Adachi, I. Tanaka, Energetics of native defects in ZnO, J. Appl. Phys. 90 (2001) 824. doi:10.1063/1.1380994.

[25] A. Janotti, C.G. Van De Walle, Oxygen vacancies in ZnO, Appl. Phys. Lett. 87 (2005) 1–3. doi:10.1063/1.2053360.

[26] M. a. Lampert, Simplified theory of space-charge-limited currents in an insulator with traps, Phys. Rev. 103 (1956) 1648–1656. doi:10.1103/PhysRev.103.1648.

[27] A. Younis, D. Chu, S. Li, Bi-stable resistive switching characteristics in Ti-doped ZnO thin films., Nanoscale Res. Lett. 8 (2013) 154. doi:10.1186/1556-276X-8-154.

[28] C. Chen, F. Pan, Z.S. Wang, J. Yang, F. Zeng, Bipolar resistive switching with self-rectifying effects in Al/ZnO/Si structure, J. Appl. Phys. 111 (2012) 013702. doi:10.1063/1.3672811.

[29] M.A. Lampert, P. Mark, Current Injection in Solids, Academic Press in New York, 1970.

[30] F.-C. Chiu, A Review on Conduction Mechanisms in Dielectric Films, Adv. Mater. Sci. Eng. 2014 (2014) 1–18. doi:10.1155/2014/578168.

[31] M. Ismail, I. Talib, C.-Y. Huang, C.-J. Hung, T.-L. Tsai, J.-H. Jieng, et al., Resistive switching characteristics of Pt/CeO_x /TiN memory device, Jpn. J. Appl. Phys. 53 (2014). doi:10.7567/JJAP.53.060303.

[32] K.A. Morgan, R. Huang, K. Potter, C. Shaw, W. Redman-White, C.H. De Groot, Total Dose Hardness of TiN/HfO_x/TiN Resistive Random Access Memory, IEEE Trans. Nucl. Sci. 61 (2014) 2991–2996. doi:10.1109/TNS.2014.2365058.